



HAL
open science

Optoelectronic sensors degradation induced by the radiations of the space environment

Christophe Inguibert, Thierry Nuns, Kevin Lemiere, Dominique Hervé, Aurélien Vriet, Juan Barbero, Juan Moreno, Alexandru Nedelcu, Samuel Ducret

► To cite this version:

Christophe Inguibert, Thierry Nuns, Kevin Lemiere, Dominique Hervé, Aurélien Vriet, et al.. Optoelectronic sensors degradation induced by the radiations of the space environment. OPTRO 2020, Jan 2020, PARIS, France. hal-02487060

HAL Id: hal-02487060

<https://hal.science/hal-02487060>

Submitted on 21 Feb 2020

HAL is a multi-disciplinary open access archive for the deposit and dissemination of scientific research documents, whether they are published or not. The documents may come from teaching and research institutions in France or abroad, or from public or private research centers.

L'archive ouverte pluridisciplinaire **HAL**, est destinée au dépôt et à la diffusion de documents scientifiques de niveau recherche, publiés ou non, émanant des établissements d'enseignement et de recherche français ou étrangers, des laboratoires publics ou privés.

Optoelectronic sensors degradation induced by the radiations of the space environment

C. Inguibert⁽¹⁾, T. Nuns⁽¹⁾, K. Lemiere⁽¹⁾, D. Hervé⁽²⁾, A. Vriet⁽²⁾, J. Barbero⁽³⁾, J. Moreno⁽³⁾, A. Nedelcu⁽⁴⁾, S. Ducret⁽⁴⁾

(1) - ONERA-DPHY, 31055 Toulouse, France (e-mail: christophe.Inguibert@onera.fr, Thierry.Nuns@onera.fr).

(2) - SODERN, 20 Avenue Descartes, 94450 Limeil-Brévannes, France (e-mail: dominique.herve@sodern.fr, aurelien.vriet@sodern.fr).

(3) - ALTER Technology, Madrid, Spain (e-mail: juan.barbero@altertechnology.com, juan.moreno@altertechnology.com)

(4) LYNRED, Avenue de la Vauve - CS20018, Palaiseau, France (e-mail: Alexandru.Nedelcu@lynred.com, Samuel.Ducret@lynred.com).

KEYWORDS: Radiation effects, image sensors, photodiodes, space

Abstract:

Space systems are subject to space radiative environment, and potentially to radiations injected in low earth orbit by the explosion of nuclear weapons. Optoelectronic components of space systems are sensitive to the radiation induced degradation of the semiconductor material. This paper presents recent results obtained during a study funded by the EDA [1] (European Defense Agency): JIP-ICET2 A-1341-RT-GP within the CapTech Technologies for Components and Modules' (TCM) in EDA. (Tracking #: SD102-11).

1. INTRODUCTION

Space system undergo particularly hard natural radiation environment, but can also potentially be subject to the radiations injected in low earth orbit by the explosion of nuclear weapons. Those radiations can cause errors in electronic systems that creates special design challenges. Preventing and reducing the susceptibility to radiation damage is thus an important issue for all space and military applications. Electronic devices are particularly sensitive to radiation effects and in order to ensure the proper operation of such systems, it is indispensable to develop a better knowledge and modeling of the radiative impacts on embedded electronic devices.

Optoelectronic components find more and more applications in space systems (imaging, attitude control, optical links for secure data transfer or electric isolation...) and involve ever new materials and alloys that have a potential interests in term of technical characteristics but may have critical degradations under a radiation constraint. The sensitivity of the new

materials is not well understood and need specific studies.

ONERA in collaboration with some other partners (SODERN, ALTER tech., SOFRADIR) has addressed this issue in the framework of a contract with the European Defense Agency (EDA) and this paper presents its main outcomes.

The study focusses on the effect of the atomic displacement produced after the high energy space and neutron particles irradiation. It concerns both the mean degradation that can be observed in single devices like photodiodes and LEDs, and the dispersion of the degradation that appears on detector arrays due to statistical effects. It proposes both experimental evaluation of detectors and LED in different III-V materials, the evaluation of imagers for star tracking applications and the modeling of the dark signal non uniformity (DSNU). The irradiation of the samples under high energy protons, neutrons, gamma rays and electrons were performed on different European facilities.

For the study of the mean degradation, some photodiodes and LED for application in the infrared, visible and UV domains have been irradiated and tested. Different materials used for each application are tested. The measurements concern the dark current increase for the detectors and the optical output power for the emitters. Some silicon image sensors operating in the visible domain have also been tested. The distribution of dark current is compared to simulation results obtained with a Monte Carlo method that have been developed.

2. RADIATION ISSUE

Energetic particles of the space environment interact with the atoms and the electrons of the irradiated material, inducing different degradation mechanisms.

Due to their functioning mode, optoelectronic devices are particularly sensitive to the defects enhancement induced by the impinging particles. The atoms of the semiconductor lattice can be displaced thanks to nuclear interactions (coulombian, nuclear inelastic) [2], [3]. These atomic displacements (interstitial/vacancy pairs) can become electrically active defects. These defects change the electrical properties of the semiconductor material (mobility of the carriers, recombination rate,...) and affect the functioning of the devices [2] [3]. Optoelectronic components, due to their specific functioning mode, are particularly sensitive to such kind of degradation mechanism [2] [3]. The defects produced consecutively to an irradiation can contribute to enhance the carriers' thermal generation rate of the depleted regions of a photodiode. The consequence is an increase of leakage current (dark current) of the p/n junctions. These phenomena contribute to increase the dark current of image sensors (CCD: Charge Coupled Device, CIS: CMOS Image Sensor) It can bring some devices, used in systems requiring a good signal-to-noise ratio, out of the specifications. Star tracking systems is a typical example. For such kind of devices evaluating the number of highly degraded pixels, hot pixels presenting a high dark current value, is of particular interest. This work addresses this issue thanks to the development of a dedicated code capable to predict the dark current distribution of irradiated imagers. The current radiation qualification procedure, in order to limit the irradiation tests, often relies on the use of such type of predicting codes. It also relies on the use of simple theoretical damage factors that allow the estimation of the degradation thanks to extrapolation procedures. Theroretical damage factors allow to predict the degradation for a given particle at a given energy when the measurements have been performed with different conditions. It allows predictions for a mission by combining the complex environment involving different species on a large energy range. In this area, the Displacement Damage Dose (DDD) [9] is used to define the radiation level in the risk assessment procedure. The DDD is a function proportional to the incident fluence of radiations (ϕ), and to the capability of the incident particles to produce defects in the target material (NIEL: Non Ionizing Energy Loss) [4][8]. The NIEL is a very useful metric, commonly employed within the radiative risk assessment procedures. It is a theoretical parameter that provides the number of atomic displacements that may be produced by unit of path length of a single incident particle. The International radiation test standards (ASTM [10], ECSS [11]) are based on the use of the NIEL parameter. The test procedures assume the proportionality between the number of atomic displacements, the number of defects and thus the measured degradation level consecutively to an

irradiation. This approach usually works. Most of the measured degradations are demonstrated to scale linearly with the NIEL [2] [3] [12], but some deviations to the so called "NIEL scaling approach" are observed from time to time [12] [13] [14]. These deviations limit the accuracy of the degradation prediction methods. This is a concern for the space applications and some improvements are required in this field. The work presented here addresses this issue. The goal here is to investigate both the sensitivity to radiations of various semiconductor materials operating in different wavelength domain and the reliability of the so called NIEL scaling approach. This study relies mostly on an important set of experimental measurements. Some specific damage calculations have also been performed for comparison.

3. EXPERIMENTAL SETUP

Different photodiodes and LEDs fabricated by different manufacturers, based on different materials, thus operating in different wavelength domains have been irradiated with particles representative of the radiative space environment. Electrons from 0.5 MeV up to 20 MeV, protons of 60 MeV, 100 MeV and 170 MeV and an atmospheric-like neutrons spectrum have been employed. Depending on the type of incident particles and energy, various deposited damage dose have been deposited ($\sim 5 \times 10^{+06}$ MeV/g up to $5 \times 10^{+09}$ MeV/g). Different damage factors have been extracted from those measurements and compared to the corresponding NIELs.

Three different silicon based image sensors have also been irradiated with protons of 60 MeV, 100 MeV and 170 MeV and an atmospheric-like neutrons spectrum.

The devices have been irradiated with protons, electrons, neutrons and gammas thanks to five different facilities. Two electron energies (0.5 and 1.5 MeV) were performed with the Van de Graaff accelerator GEODUR of ONERA (Toulouse, France) [15]. Three higher electron energies (6 MeV, 12 MeV and 20 MeV) were performed at the RADEF facility (LINAC of the University of Jyväskylä, Finland) [16]. Some devices have also been irradiated with protons of 60 MeV, 100 MeV, and 170 MeV, as well as with the atmospheric-like neutron spectrum of The Svedberg Laboratory (TSL, Uppsala, Sweden) facility [17]. The PAULA facility (Proton fAcility in Uppsala). Provides a Quasi-Monoenergetic proton beam while the ANITA facility (Atmospheric-like Neutrons from thlck Target) provides a continuous spectrum ranging from thermal energies up to ~ 180 MeV. The devices have also been irradiated at the CAN-RADLAB laboratory (National Centre for Accelerators [18]), using a Cobalt-60 source placed into a Gammabeam@X200 irradiator. Those gamma photon irradiations

have demonstrated that all these devices have a low sensitivity to ionizing dose effects. All the measured degradations are dominated by the DDD allowing us to interpret confidentially the data in term of displacement damage effects.

Table 1 : List of tested devices (LEDs and photodiodes).

Manufacturer	Reference	material	Lambda (nm)
LEDs			
SETI	UVTOP255-FWTO18	AlGaIn	255
Vishay	VLMK33R1S2	AllnGaP	617
Roithner	LED1550-35	InGaAsP	1550
	UVled370-110e	AlGaIn	375
Kyosemi	kede 1552	InGaAsP	1550
Photodiodes			
Roithner	GUVV-T10GD	InGaIn	400
Kyosemi	KPDU37H1		
Jenoptik	EPD-525	GaP	200-550
Hamamatsu	G1963		
Excelitas	C30618	InGaAs	1000-1700
OSI	FCI Q1000		
Sofradir	Snake		

Table 2: List of tested image sensors.

Manufacturer	reference	Pixel pitch
CMV2000	CMOSIS	5.5 μm
HAS2	On Semi.	18 μm
Python		4.8 μm

4. RESULTS

4.1. LEDs

Both the change in the optical power and a drift on the I(V) forward characteristics of LEDs have been studied. The emission spectrum has also been recorded. The I(V) characteristics of most of the LEDs do not depict any significant change, neither the emission spectrum. But the output power is demonstrated to decrease after the irradiations. The relative decrease depends on the material. The Figure 1 Figure 2, Figure 3 Figure 4 Figure 5 shows the relative output power as a function of the displacement damage dose for the 5 LEDs after protons and electron irradiations. The InGaAsP LEDs are the most sensitive to DDD, and one can see that the output power is very low after irradiation (less than 20% after a DDD of 8 MeV/g). The less sensitive are the AlGaIn devices (20% of power loss after almost a DDD of

10 MeV/g). The results do not seem to be bias dependent. The only material type that may exhibit a bias effect is the InGaAIP. Finally, some discrepancies may appear when comparing the different types of irradiation (for example the different proton energies). This may be due a lack of accuracy of the NIEL evaluation.

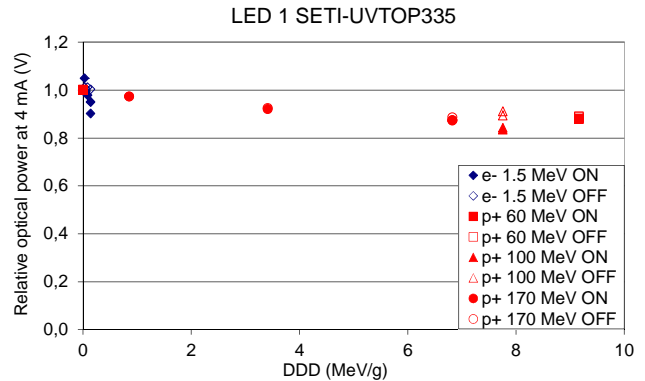


Figure 1: Relative output power loss of the SETI LED after irradiation as a function of the DDD.

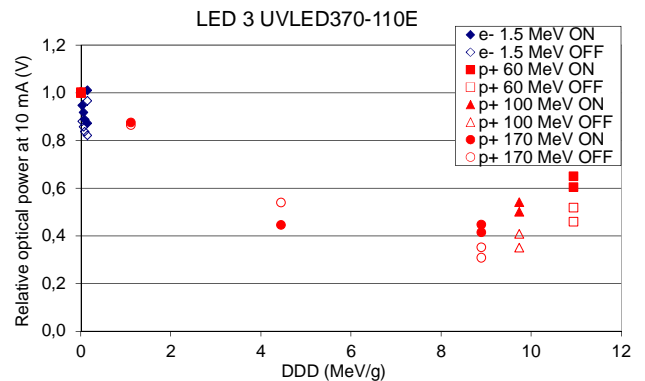


Figure 2: Relative output power loss of the Roithner 370 LED after irradiation as a function of the DDD.

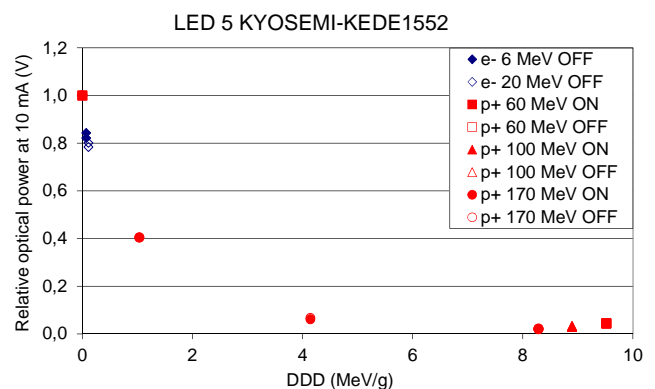


Figure 3: Relative output power loss of the Kyosemi 370 LED after irradiation as a function of the DDD.

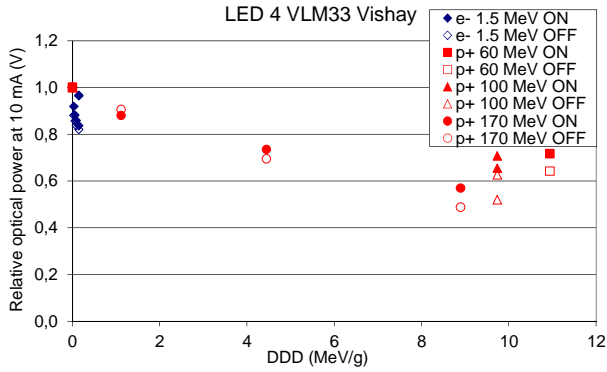


Figure 4: Relative output power loss of the Vishay 370 LED after irradiation as a function of the DDD.

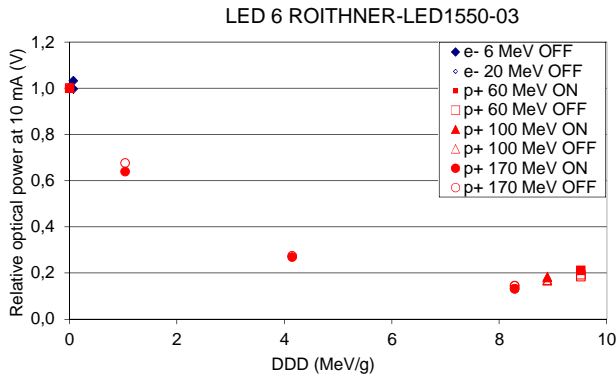


Figure 5: Relative output power loss of the Roithner1550 LED after irradiation as a function of the DDD.

4.2. Photodiodes

Seven photodiodes coming from seven different manufacturers (Roithner, Kyosemi, Jenoptik, Hamamatsu, Excelitas, OSI, and Lynred) have been tested during the irradiation campaigns. The Roithner and Kyosemi devices are InGaN photodiodes operating typically at 400 nm, Jenoptik and Hamamatsu are GaP photodiodes operating in the range [200 nm, 500 nm], the other are InGaAs photodiodes operating beyond 1000 nm.

Large gap materials photodiodes (InGaN, GaP) are demonstrated to be less sensitive to radiation than small gap materials (InGaAs-1.1 eV) due to the fact that, at a given temperature, the defects in a larger gap are less effective to produce a thermal current. The analysis has been focused on InGaAs photodiodes that present the most important susceptibility to radiation damage. Lynred [19] provided specific test vehicles of the SNAKE device which is an array of InGaAs PIN photodiodes operating in the 0.9 μm to 1.7 μm wavelength domain. The test vehicles consist in a set of circular single

photodiodes of different dimensions (diameter in the range [4 μm , 300 μm]) and 10x10 sub-arrays of pixels with various pitches (in the range [10 μm , 30 μm]) where all pixels are addressed in parallel. A maximum of six different elements, selected within the available topologies of the test vehicles, have been measured during this study. Two other InGaAs devices have been tested. The PIN photodiode C30618 from Excelitas [20] and the FCIQ1000 from OSI [21]. Excelitas device is designed for use in OEM fiber-optics communications systems and high-speed receiver applications. It operates between 1000 nm and 1600 nm and has a diameter of 350 μm and a maximum intrinsic dark current of typical ~ 1 nA with an applied voltage of -10 V (the bias at which the current measurements were made). The OSI photodiode is segmented into four quadrants with a full active area of 1000 μm diameter and presents a 0.5 nA dark current at -5 V (bias for the current measurements). The Q1000 photodiode is optimized for a good responsivity from 1100 nm to 1620 nm.

The increase in dark current of photodiodes is proportional to the number of defects N_t :

$$\text{Eq. 1} \quad \Delta J_{\text{Dark}} = n_i \cdot \sigma \cdot v_{\text{th}} \cdot \Delta N_t (\Phi)$$

Where ϕ is the incident fluence, σ , the capture cross section of the defect, n_i the density of intrinsic carrier and v_{th} the thermal velocity of the carriers. The amount of produced defects after irradiation is equal to ΔN_t . It is proportional to the NIEL and to the incident fluence (DDD).

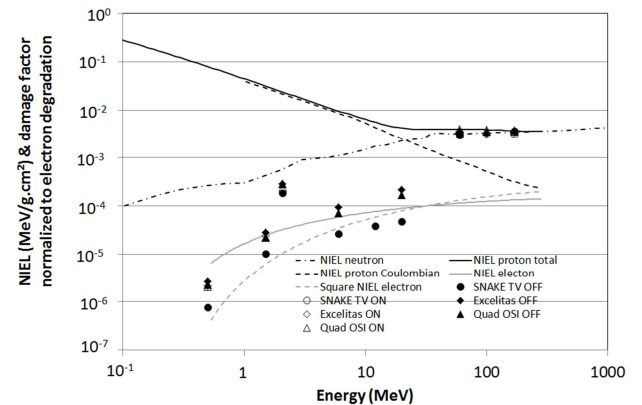


Figure 6: Comparison of experimental InGaAs damage factors measured in OSI, Excelitas, and Lynred devices with theoretical NIEL.

The voltage applied on the photodiodes have been chosen in order to be in a full depleted regime dominated by this generation current. No significant differences have been observed between the devices that have been biased and shorted during the irradiations. The electrical measurements and the irradiations have been performed at ambient

temperature (~24°C). The measurements have been performed at different annealing times. Two months storage at room temperature shows negligible impact of the annealing processes (~10% recovery).

All tested photodiodes have depicted a linear dark current variation as a function of the incident fluence allowing a reliable extraction of damage factors. These damage factors have been plotted as a function of the energy of the incident particles and compared to the theoretical NIEL.

First of all, one can notice the overall good agreement between the NIEL and the experimental data. The so called "NIEL scaling" approach is validated at first order for InGaAs material. For protons the energy dependence of the experimental damage factors is consistent with the NIEL. For electrons the dependence with the NIEL is not linear but "quadratic". i. e., the damage factor is not an affine function of the NIEL, but a power of two function. This behavior is identical for all the tested references. It is in line with previous observations made for Si and GaAs [2] [14][22]. The discrepancy observed between experimental damage factors for electrons does not necessarily deal with electrons. It is the consequence to the normalization that has been performed relatively to proton data. At this stage, a discrepancy can be noticed, but it is not possible to attribute this effect to a particle type or another. The underestimation of the degradation by the neutron NIEL could be attributed to the uncertainty in the definition of the equivalent damage fluence of the ANITA neutron spectrum. The equivalent damage energy of 2.07 MeV, calculated for InGaAs is subject to the accuracy of both the definition of the ANITA spectrum, and of the neutron InGaAs NIEL.

4.3. Image sensors

The radiation damage processes are stochastic and after studying the average degradation levels on isolated photodiodes, it is interesting to study the effect of inhomogeneities on the large set of photodiodes that represents a CMOS imager. Indeed, the damage level produced by an irradiation is not homogeneous through the array, but on the contrary, fluctuates from a pixel to another. The induced global damage distribution over the pixels array (DCNU) is the combination of the damage produced by individual interactions, that change from an interaction to another, "weighted" by the probability distributions (Poisson, normal) governing the statistic of the number of interactions per pixel. Some defective pixels that significantly deviate from the average behaviour of their neighbours can be troublesome for some applications such as star trackers. The presence of highly degraded pixels, presenting high dark current

values reduce the performances of the attitude control systems where Image sensors can be used. These bright pixels, known as "hot" pixels, can be mixed with real stars, and slow down the stabilization of the satellite attitude. The image sensors are nowadays becoming more popular thanks to their low-power, low-cost and high-integration capabilities. They are currently used in machine vision, security and surveillance, scientific imaging and of course in aerospace and defense applications where imaging sensors can face harsh radiative environments. Protons are particularly troublesome because, unlike electrons, they initiate nuclear reactions that produce high energy recoil nuclei (>1 MeV), able to generate high degradation levels of pixel properties.

DCNU calculation

Hence, the dispersion of the degradation from a pixel to another cannot be determined thanks to the NIEL which provides only an average degradation. Actually, a different number of interactions is produced in each pixel, and each interaction produces a different number of defects, resulting in a wide range of damage from a pixel to another. This random process which is governed by a Poissonian law can be modelled thanks to a Monte Carlo method. This issue has been addressed thanks to the development of a Monte Carlo code based on the GEANT4 library [23]. GEANT 4 is a C++ toolkit assembled by an international collaboration, for describing radiation interaction with matter [23]. It allows the transport of radiation in complex 3D geometries and handling physical parameters such as ionizing and non-ionizing deposited energy. An application, based on that library, has been developed in order to calculate the damage produced in the depleted regions of a defined array of pixels, where the thermal generation should occur. The method is based on the following algorithm.

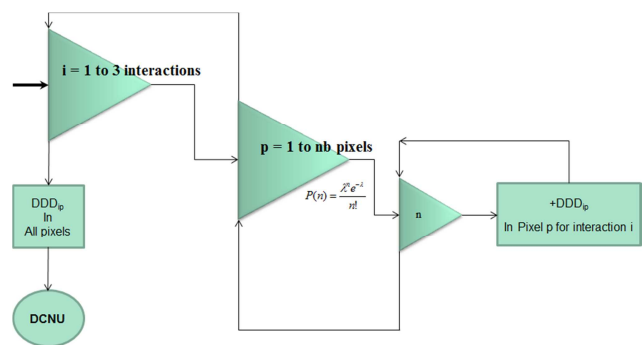


Figure 7: Algorithm of the Monte Carlo approach.

The principle of the calculation is as follow. For each type of interactions the contribution to the DCNU is evaluated according to a similar process. For a given pixel and a given type of interaction:

- 1- The number of interaction is randomly selected in a Poisson's law,
- 2- The damage produced by each interaction is calculated,
- 3- The total damage is the sum of the degradation induced by individual interactions,
- 4- The corresponding dark current is calculated assuming that it is proportional to the number of atomic displacements.

For the 3 types of interactions able to produce damage (Coulombian nuclear elastic and nuclear inelastic), the damage produced by individual interactions is calculated with different methods. The coulombian contribution is evaluated thanks to known analytical expressions [7]. On a contrary, a dedicated GEANT4 application toolkit has been developed for both nuclear elastic and inelastic interactions. The nuclear elastic and inelastic interactions are able to produce recoil nuclei of several MeV that can travel several tens of micrometers in silicon. These recoil nuclei can come from neighbours' pixels or surrounding dead zones and degrade the studied depleted region. The GEANT4 application allows taking into account these border effects. A database of damaged pixels is fulfilled which then is used to compute the dark current distribution during a second phase. The final DCNU is calculated during this second phase by combining the degradation induced by several different interactions randomly selected in the databank or calculated analytically for Coulombian interactions. A full description of this method can be found in refs. [24][26].

The dark current distributions have been calculated for the different tested devices.

Tested devices

Three commercial silicon devices have been tested. HAS2 and Python form On Semiconductor, and CMV2000 from CMosis. The devices are briefly described in the following.

HAS2: The Accuracy STR 2 sensor (HAS2) is a 1024 x 1024 pixel rolling shutter Active Pixel Sensor (APS), featuring a programmable (gain and offset) output amplifier (PGA) and an internal 12 bits ADC. The CMOS image sensor was designed and manufactured by ON Semiconductor under ESA contract

17235/03/NL/FM for star tracker applications. Pixel design is based on a photodiode coupled with a three transistor readout circuit. The HAS2 is the descendant from a lineage radiation-hardened by design sensors from ON Semiconductor: the photodiodes include a doped surface protection layer to prevent the depleted area from reaching the field oxide interface, while the CMOS readout circuitry is designed using enclosed geometry transistor layouts.

PYTHON: The PYTHON5000 is a 4.8 μm global shutter CMOS Image Sensors designed by On Semiconductor. It offers a resolution of 2592 x 2048 pixels.

CMV2000: The CMV2000 is a 5.5 μm pitch, global shutter CMOS Image Sensors designed by CMOSIS. CMV2000 offer a resolution of 2048 x 1088 pixels, with 8 transistors per pixel. The CMV2000 is produced on the 0.18 μm CIS process from TowerJazz. Microlenses present on the pixels are 550 nm thick, and made in PMMA (Poly(methyl methacrylate)). The test conditions are summarized in the following table.

Table 3: Image sensors test conditions (in grey) with the different applied fluences in particles/cm²

	Neutron 14 MeV	Neutron Anita	Proton 60 MeV	Proton 170 MeV
HAS2	2.4 10 ⁺¹⁰	5.23 10 ⁺⁰⁹		
Python			1. 10 ⁺¹¹ 3. 10 ⁺¹⁰ 1. 10 ⁺¹⁰	4.96 10 ⁺¹¹ 1.66 10 ⁺¹¹ 4.96 10 ⁺¹⁰ 1.66 10 ⁺¹⁰
CMV2k	2.4 10 ⁺¹⁰	5.23 10 ⁺¹⁰		4.96 10 ⁺¹¹ 1.66 10 ⁺¹¹ 4.96 10 ⁺¹⁰ 1.66 10 ⁺¹⁰

Results

Some comparisons of simulated DCNU with experimental measurements are shown in the following figures.

The Figure 8 shows simulation results of the DCNU of Python device for various applied fluences. We can see the evolution of the DCNU. The number of highly degraded pixels increases at the expense of the number of weakly degraded pixels. The maximum of the distribution is shifted towards higher values with increasing fluences. These observations are similar for the two different energies (58.5 MeV, and 169.5 MeV). On Figure 9 Figure 10 the comparisons with experimental measurements are quite satisfactory for protons of 58.5 MeV and 169.5 MeV.

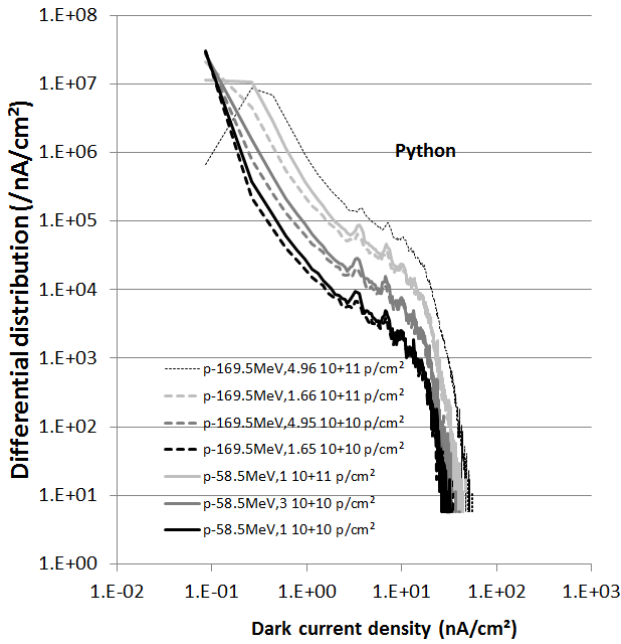


Figure 8: DCNU calculated with the Monte Carlo method for the various test conditions of the Python device (54.9 MeV and 169.5 MeV protons with various fluences).

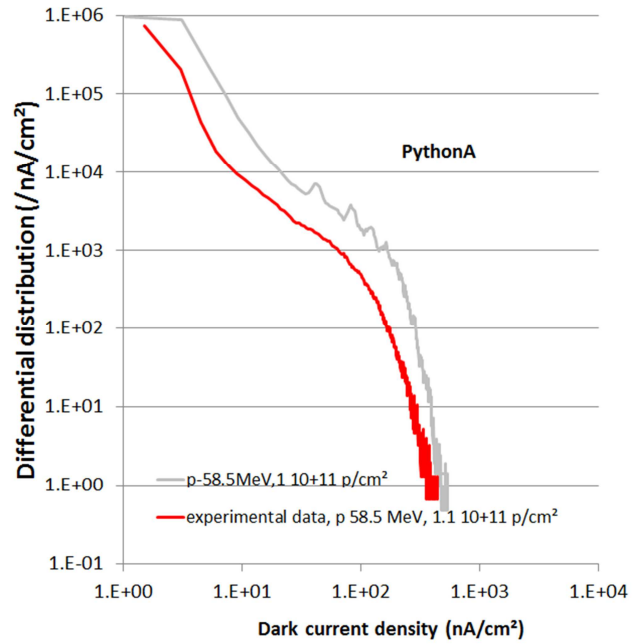


Figure 10: Comparison of calculated DCNU with the measurements for the Python device irradiated with 58.5 MeV protons at a fluence of 10^{+11} p/cm².

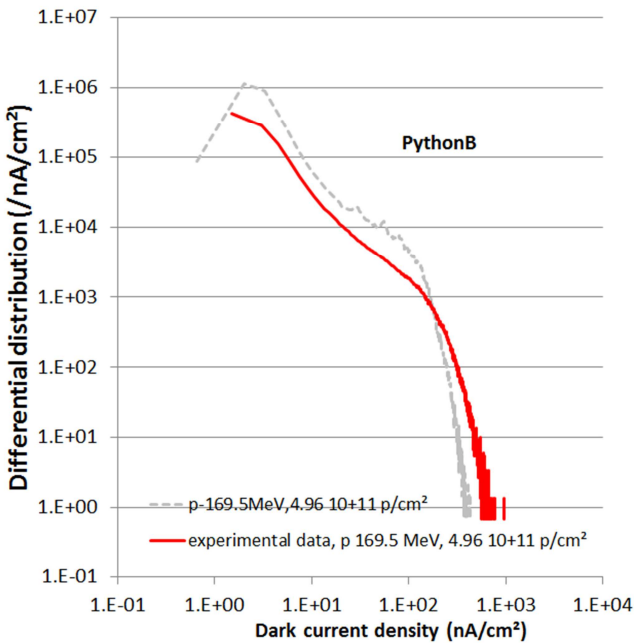


Figure 9: Comparison of calculated DCNU with the measurements for the Python device irradiated with 169.5 and 58.5 MeV protons at a fluence of $4.96 \times 10^{+11}$ p/cm².

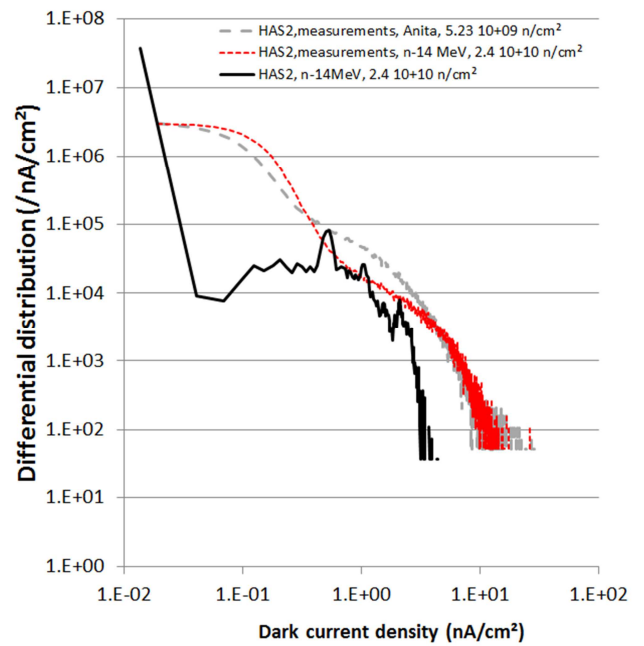


Figure 11: Comparison of calculated DCNU with the measurements for the HAS2 device irradiated with Anita spectrum and 14 MeV neutrons.

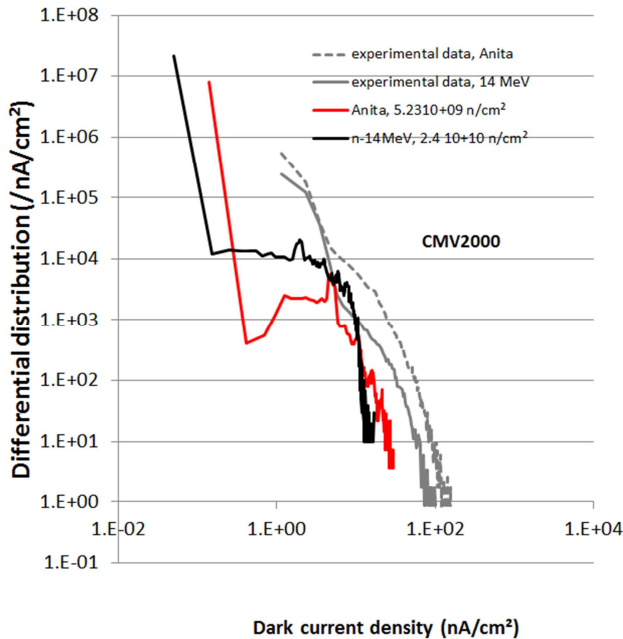


Figure 12: Comparison of calculated DCNU with the measurements for the HAS2 device irradiated with Anita spectrum and 14 MeV neutrons.

The agreement between simulations and experiment is clearly worse for neutrons. As can be seen in Figure 11 Figure 12 for HAS2 and CMV2000 devices the simulations underestimate significantly the degradation. In addition the experimental DCNU shows a significantly smoother behavior. The simulations predict a significant number of not degraded pixels while the experimental data show a continuous number of degraded pixels down to very low damage levels. The damage level induced by neutrons is quite low and is still strongly driven by the initial dark current level before irradiations. The simulations do not take this into account and only show a dark current increase DCNU. Within the simulations, the pixels are taken blanked of defects, that is clearly not the case in the reality. To improve our prediction the initial dark current distribution shall be included in the calculation.

5. CONCLUSION

The study has highlighted different phenomenon. First of all, the NIEL scaling approach commonly used in the space community has been validated for InGaAs material. Contrary to other materials operating in UV and visible domain, this low gap material operating in the infrared domain is shown to present a quite strong sensitivity to radiations. Similar deviations observed for Si and GaAs are observed for incident electrons.

The dependence of measured degradation level to NIEL seems to be quadratic.

The comparisons of DCNU Monte Carlo simulations with experimental measurements performed on three different image sensors irradiated with various conditions including protons and neutrons are variable. The agreement is quite good for protons and some significant deviations are observed for neutrons that are attributed to the fact that initial dark current distributions are neglected in the simulations. To improve our DCNU different mechanisms shall be added:

- Electric field enhancement of generation centers,
- Recombination effects,
- Taking into account the nature of produced defects.

Finally the Monte Carlo simulations have allowed us to interpret some deviations of the NIEL scaling method as a statistical artefact induced by the stochastic nature of the deposition of the displacement damage dose [27]. This new understanding of the damaging processes is an important outcome of the combined analysis of the DCNU and the III-V semiconductor degradation proposed in this work. However, the full validation of this new interpretation of some data shall be performed thanks to specific irradiation tests, complementary to, that have been performed during this study.

6. REFERENCES

- [1] The European Defence Agency [Online]. Available: <https://www.eda.europa.eu/> Accessed July 27, 2019.
- [2] Srour J. R. (2003) Review of displacement damage effects in silicon devices, *IEEE Trans. Nucl. Sci.*, **50**(3), 653–670.
- [3] Srour J. R., Palko J. W. (2006) A framework for understanding displacement damage mechanisms in irradiated silicon devices, *IEEE Trans. Nucl. Sci.*, **53**(6), 3610-3620
- [4] Messenger S. R., Burke E. A., Summers G. P., Xapsos M. A., Walters R. J., Jackson E. M., and Weaver B. D. (1999) Non ionizing energy loss (NIEL) for heavy ions, *IEEE Trans. Nucl. Sci.*, **46**(6), 1595–1602.
- [5] Akkerman A., Barak J., Chadwick M. B., Levinson J., Murat M., and Lifshitz Y. (2001) Updated NIEL calculations for estimating the damage induced by particles and gamma-rays in Si and GaAs, *Rad. Phys. and Chem.*, **62**, 301–310.
- [6] Jun I., Kim W., and Evans R., (2009) Electron nonionizing energy loss for device applications, *IEEE Trans. Nucl. Sci.*, **56**(6), 3229–3235.

- [7] Inguibert C., and Gigante R. (2006) NEMO: A code to compute NIEL of protons, neutrons, electrons, and heavy ions, *IEEE Trans. Nucl. Sci.*, **53**(4), 1967–1972.
- [8] Boschini M. J., Consolandi C., Gervasi M., Giani S., Grandi D., Ivanchenko V., Nieminen P., PenBOtti S., Rancoita P. G., Tacconi M., E. ESA, and A. G. Noordwijk, (2010) Nuclear and non-ionizing energy-loss for Coulomb scattered particle from low energy up to relativistic regime in space radiation environment,” in *Proc. the 12th ICATPP Conference on Astroparticle, Particle, Space Physics and Detectors for Physics Applications*, Como, Italy, 9–23.
- [9] Inguibert C., Messenger S. (2012) Equivalent Displacement Damage Dose for On-Orbit Space Applications, *IEEE Trans. Nucl. Sci.*, **59**(6), 3117–3125.
- [10] ASTM E722-14, (2014) Standard Practice for Characterizing Neutron Fluence Spectra in Terms of an Equivalent Monoenergetic Neutron Fluence for Radiation-Hardness Testing of Electronics, ASTM International, West Conshohocken PA, 1-18.
- [11] ECSS, “European cooperation for space standardization,” <<https://ecss.nl/home/ecss-a-single-set-of-european-space-standards/>>, (01 April 2019).
- [12] Arnolda P., Inguibert C., Nuns T., Boatella-Polo C. (2011) NIEL scaling: comparison with measured defect introduction rate in silicon, *IEEE Trans. Nucl. Sci.*, **58**(3), 756–763.
- [13] Summers G. P., Burke E. A., Shapiro P., Messenger S., and Walters R. J., (1993) Damage correlations in semiconductors exposed to gamma, electron and proton radiations, *IEEE Trans. Nucl. Sci.*, **40**(6), 1372–1379.
- [14] Messenger S. R., Walters R. J., Burke E., Summers G. P., and Xapsos M. A., (2001) NIEL and damage correlations for high-energy protons in gallium arsenide devices, *IEEE Trans. Nucl. Sci.*, **48**(6), 2121–2126.
- [15] GEODUR: Chambre d'irradiation électrons multi applications (matériaux, composants, charge interne des isolants. [Online]. Available: <http://www.onera.fr/fr/desp/geodur> Accessed July 27, 2017.
- [16] RADEF: Jyväskylän Yliopisto, University of Jyväskylä. [Online]. Available: <https://www.jyu.fi/fysiikka/en/research/accelerator/radef>. Accessed July 27, 2017.
- [17] The ANITA neutron beam facility [Online]. Available: http://www.tsl.uu.se/irradiation-facilities-tsl/ANITA_neutron_beam_facility/ Accessed July 27, 2017.
- [18] CAN: Centro Nacional de Aceleradores [Online]. Available: <http://www.centro.us.es/cna/index.php/en/facilities/co-60-irradiator> Accessed April 10, 2019.
- [19] LYNRED: Lynred [Online]. Available: <https://www.lynred.com> Accessed September 10, 2019; notice that Sofradir became Lynred in 2019.
- [20] EXCELITAS: Excelitas technologies. [Online]. Available: <http://www.excelitas.com/Pages/Index.aspx> Accessed July 27, 2017.
- [21] OSI: OSI Optoelectronics. [Online]. Available: <http://www.osioptoelectronics.com/standard-products/silicon-photodiodes.aspx> Accessed July 27, 2017.
- [22] EL Allam E., Inguibert C., Nuns T., Meulemberg A., Jorio A., Zorkani I., (2017) Gamma and Electron NIEL Dependence of Irradiated GaAs, *IEEE Trans. Nucl. Sci.*, **64**(3), 991–998.
- [23] Agostinelli S. et al., (2003) Geant 4 a simulation toolkit, *Nucl. Instrum. Methods Phys. Rev. A*, **A506**, 250-303
- [24] Inguibert C., Nuns T., Ursule M. C., Falguère D., Hervé D., Beaumel M., Poizat M., (2014) Modeling the Dark Current Non-Uniformity of Image Sensors With GEANT4, *IEEE Trans. Nucl. Sci.*, **61**(6), 3323–3330.
- [25] Ursule M.C., Inguibert C., Nuns T., (2016) Impact of the border crossing effects on the DCNU for pixels arrays irradiated with high energy protons, *IEEE Trans. Nucl. Sci.*, **63**(4), 2159-2167.
- [26] Ursule M. C.; Inguibert C. ; Nuns T. ;Morio J., (2018) Comparison of Methods to Calculate the Dark Current Non uniformity, *IEEE Trans. Nucl. Sci.*, **65**(7), 1345–1354.
- [27] Inguibert C., Nuns T. (2018) About the scatter of displacement damage and its consequence on the NIEL scaling approach, In *Proc. RADECS2018 Conference Goteborg*.